Traffic 2012; **13:** 1083–1089

doi:10.1111/j.1600-0854.2012.01369.x

Botulinum Neurotoxin A Impairs Neurotransmission Following Retrograde Transynaptic Transport

Laura Restani[1], Elena Novelli[2], David Bottari[1], Paola Leone[2], Ilaria Barone[1], Lucia Galli-Resta[1], Enrica Strettoi[1] and Matteo Caleo[1,*]

[1] *CNR Neuroscience Institute, via G. Moruzzi 1, Pisa, 56124, Italy*
[2] *Fondazione G.B. Bietti, via Livenza 3, Roma, 00198, Italy*

**Corresponding author : Matteo Caleo, caleo@in.cnr.it*

The widely used botulinum neurotoxin A (BoNT/A) blocks neurotransmission via cleavage of the synaptic protein SNAP-25 (synaptosomal-associated protein of 25 kDa). Recent evidence demonstrating long-distance propagation of SNAP-25 proteolysis has challenged the idea that BoNT/A remains localized to the injection site. However, the extent to which distant neuronal networks are impacted by BoNT/A retrograde trafficking remains unknown. Importantly, no studies have addressed whether SNAP-25 cleavage translates into structural and functional changes in distant intoxicated synapses. Here we show that the BoNT/A injections into the adult rat optic tectum result in SNAP-25 cleavage in retinal neurons two synapses away from the injection site, such as rod bipolar cells and photoreceptors. Retinal endings displaying cleaved SNAP-25 were enlarged and contained an abnormally high number of synaptic vesicles, indicating impaired exocytosis. Tectal injection of BoNT/A in rat pups resulted in appearance of truncated-SNAP-25 in cholinergic amacrine cells. Functional imaging with calcium indicators showed a clear reduction in cholinergic-driven wave activity, demonstrating impairments in neurotransmission. These data provide the first evidence for functional effects of the retrograde trafficking of BoNT/A, and open the possibility of using BoNT/A fragments as drug delivery vehicles targeting the central nervous system.

Key words: retinal waves, rod bipolars, SNAP-25, synaptic blockade, transcytosis, visual system

Received 16 February 2012, revised and accepted for publication 17 April 2012, uncorrected manuscript published online 20 April 2012, published online 9 May 2012

Botulinum neurotoxins (BoNTs) are produced by anaerobic bacteria of the genus *Clostridium* and are the most potent toxins known (1,2). Seven serotypes of BoNTs exist, indicated with letters from A to G. BoNTs are metalloproteases that specifically cleave essential protein components of the neuroexocytosis machinery, the SNARE (soluble *N*-ethylmaleimide-sensitive factor attachment protein receptor) proteins (2,3). In particular, BoNT/A cleaves SNAP-25 (synaptosomal-associated protein of 25 kDa) and exerts a long-lasting blockade of synaptic transmission at peripheral and central synapses (2,4–6). Biopharmaceutical preparations of BoNT/A are increasingly being used in clinical neurology for the treatment of several neuromuscular and autonomic disorders characterized by hyperexcitability of peripheral nerve terminals (including dystonia, spasticity and hyperhydrosis) (5,7–9). BoNT/A is an excellent drug for the treatment of such pathologies, but much remains to be understood about the potential central effects of this toxin. Several studies have documented central effects of BoNT/A following peripheral application, particularly when high doses are employed (10–13). The mechanisms underlying these central actions are not well understood (14,15). Theoretically, BoNT/A applied in the periphery could produce central effects directly (via axonal transport), or indirectly, by altering sensory inputs to the brain (14–16).

Recently, we and others have demonstrated SNAP-25 cleavage in brain areas that are connected with the injection site, indicating BoNT/A retrograde axonal transport and transcytosis (10,17). However, the functional consequences of SNAP-25 proteolysis in distant areas have not been examined. Here we exploit the well-described anatomical and functional properties of the rat visual pathway to gain insight into the pathways and physiological relevance of BoNT/A trafficking in neurons. We demonstrate for the first time the impairments in neurotransmission in synapses distant from the administration site.

Results

We have previously shown that application of BoNT/A into the rat optic tectum results in retrograde axonal transport of the catalytically active protease, with SNAP-25 cleavage in synaptic terminals of amacrine cholinergic neurons impinging on retinal ganglion cells (10). We first confirmed by immunoblotting the appearance of SNAP-25 cleavage in the retina, using an antibody that is highly specific for BoNT/A-truncated SNAP-25 (10,17,18) (Figure 1A,B). Next, we asked whether BoNT/A can undergo additional cycles of retrograde transport and transcytosis that further expand the toxin spread away from the injection site. Three to fifteen days following BoNT/A injection into the tectum, we found that rod bipolar cells and phoreceptors, that are at least two synapses away from the injection site, were immunoreactive for BoNT/A-cleaved SNAP-25 (Figure 1A,C). Stained photoreceptors were unambiguously identified by their location within the outer nuclear layer (ONL) of the retina (Figure 1C). A subset of rod bipolar cells (identified by their specific marker

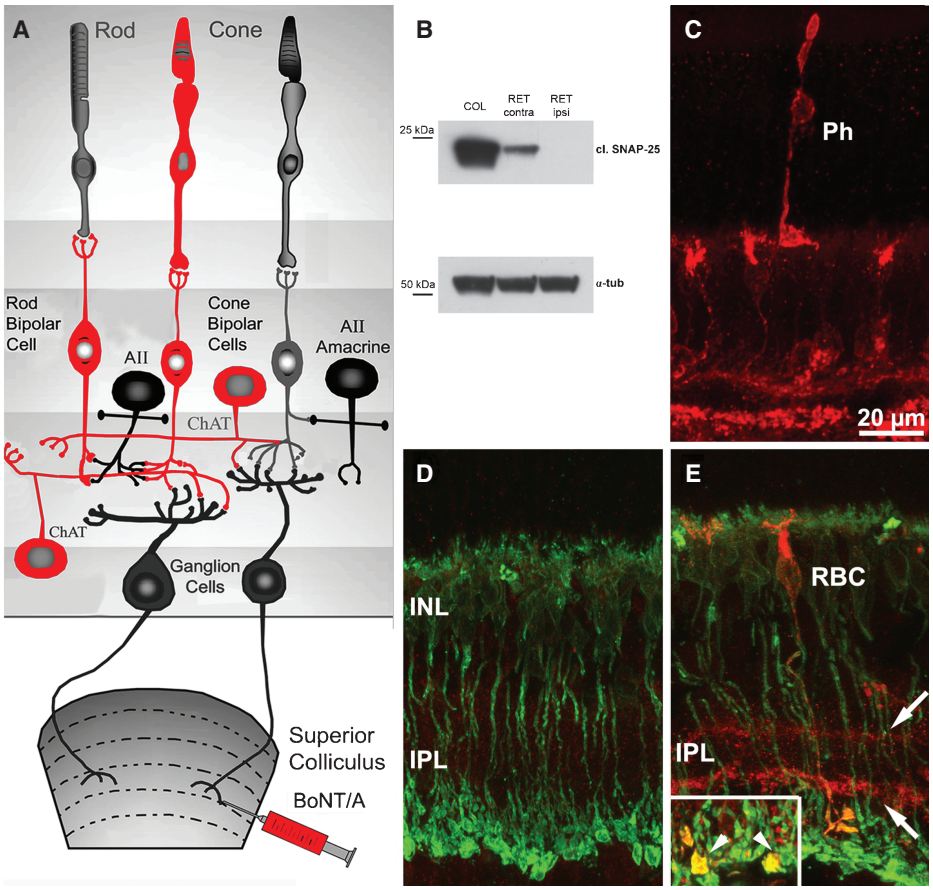

Figure 1: BoNT/A effects propagate two synapses away from the injection site. A) Simplified scheme of retinal circuitry. In red, cell types that express cleaved SNAP-25 after BoNT/A delivery to the tectum. B) Immunoblotting for cleaved SNAP-25 (cl. SNAP-25) on protein extracts from the injected colliculus (COL) and the contralateral (contra) and ipsilateral (ipsi) retina (RET). Note SNAP-25 cleavage in the retina contralateral to toxin delivery. α-tubulin (α-tub), internal standard. C) Transverse retinal section showing SNAP-25 cleavage (red) 15 days following tectal injection of BoNT/A. Note intense staining in the inner plexiform layer (IPL) and a labelled photoreceptor (Ph). D and E) Double labelling for BoNT/A-cleaved SNAP-25 (red) and protein kinase C (a rod bipolar cell – RBC - marker, green). No staining for truncated SNAP-25 is found in an animal injected with BoNT/A into the frontal cortex (D). INL, inner nuclear layer. In (E), double labelling of a RBC and its synaptic terminals in a rat with tectal delivery of BoNT/A. Arrows indicate cholinergic bands in the ON and OFF sublaminae of the IPL. Scale bar as for (C). Inset: arrowheads point to two PKC/cleaved SNAP-25 positive synaptic endings of RBCs showing a larger than normal size (twice the magnification of panel E).

protein kinase C) were also immunopositive for BoNT/A-truncated SNAP-25 (Figure 1E). Muller glial cells were not labelled, ruling out aspecific, non-synaptic uptake of the toxin. No staining was found in the retina of untreated animals or animals injected with BoNT/A into the frontal cortex (Figure 1D), indicating that retinal effects are not secondary to systemic spread of BoNT/A via the blood or cerebrospinal fluid. Thus, BoNT/A-induced SNAP-25 cleavage can be found at least two synapses away from the injection site.

The occurrence of cleaved SNAP-25-positive neurons located at least two synaptic stations away from the tectum was not occasional. Indeed, about one-third of all the labelled cells 3–15 days following injection could be identified either as rod bipolar cells or as photoreceptors (Figure 2). These neuronal types do not establish connections with ganglion cells and therefore can receive the toxin only through retinal circuits involving amacrines and cone bipolars (19–21) (Figure 1A).

We next examined whether SNAP-25 cleavage is associated with morphological abnormalities in the synaptic terminals of retrogradely intoxicated neurons. Confocal analysis of synaptic boutons in control (cleaved SNAP-25-negative) and intoxicated (cleaved SNAP-25-positive) rod bipolar cells within the same retina demonstrated a clear enlargement of synaptic terminals containing BoNT/A-truncated SNAP-25 with respect to controls (Figure 3A). The increase in terminal size was significant 3 days after tectal injection of BoNT/A (BoNT/A 3 days versus control, K-S test, $p < 0.05$; Figure 3A) and was further enhanced at 15 days (K-S test, BoNT/A 15 days versus control, $p < 0.001$; Figure 3A), suggesting

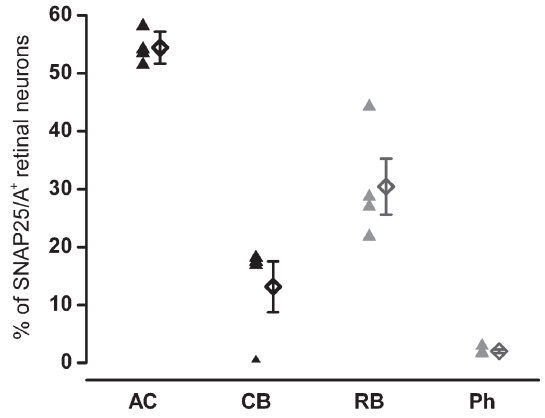

Figure 2: Retrograde BoNT/A targets different types of retinal neurons. Relative proportions of cleaved SNAP-25-positive (SNAP25/A$^+$) neurons in the retina after tectal delivery of BoNT/A. SNAP25/A$^+$ neurons were divided into four classes: rod bipolars (RB, PKC positive), cone bipolars (CB, PKC negative), amacrine cholinergic cells (AC) and photoreceptor cells (Ph), the latter two identified on the basis of their position and typical morphology. Each triangle represents the percentage obtained in a single rat; diamonds indicate the average (±SE) per class. In total, 416 cells were scored from four animals. Black triangles indicate cells impinging directly on retinal ganglion cells; grey triangles refer to cell types located at least two synapses away from the tectum. Note that about one-third of the SNAP25/A$^+$ neurons are located two synapses away from the injection site.

a progressive cumulative effect. Electron microscopy analysis revealed the appearance of enlarged rod bipolar cell endings in animals with tectal injections of BoNT/A (Figure 3B,C). Although we were unable to determine whether these swollen terminals contain cleaved SNAP-25, they were never encountered in control retinas, and most likely correspond to the enlarged boutons seen by confocal microscopy in BoNT/A-treated samples. The enlarged terminals were filled with an abnormally high number of synaptic vesicles (Figure 3B). Both the enlargement of synaptic boutons of rod bipolar cells and the increase in the total number of synaptic vesicles are strong indicators of impairments in neuroexocytosis following retrograde transynaptic transport of BoNT/A from the injection site.

To directly document distant functional changes in neurotransmission after tectal BoNT/A, we focused on cholinergic amacrine cells, because this is the population of retinal neurons with the highest proportion of cleaved SNAP-25-positive cells (10) (Figure 2). A well-known function of the cholinergic neurons is that they generate spontaneous activity during retinal development (22–26). Thus, if SNAP-25 cleavage in these neurons corresponds to functional deficits in cholinergic transmission, this should be evident from recordings of retinal spontaneous activity in neonatal rats.

We performed BoNT/A injections into the superior colliculus of P0–P2 rat pups and we consistently found immunolabelling for cleaved SNAP-25 in cholinergic, 'starbust' amacrine cells (Figure 4A). No labelling was found in the retina of pups injected with BoNT/A into the frontal cortex, again arguing against passive spread of BoNT/A (Figure 4B).

Spontaneous retinal activity in the first postnatal week consists of rhytmic 'waves' of activity spreading across the retina, which are completely abolished by cholinergic antagonists (22–26). Thus, we exploited retinal waves as a functional readout of acetylcholine release from starbust cells. Using calcium indicators, we imaged retinal waves in retinas from control pups and pups with tectal BoNT/A injection, 2–5 days after toxin application. We found a very significant decrease in wave frequency in BoNT/A-treated samples as compared to controls (Figure 4C,D; *t*-test, $p < 0.001$). Furthermore, in retinas from injected animals wave frequency was inversely correlated with the number of starbust cells immunopositive for cleaved SNAP-25 (Figure 4E). These data provide a strong indication of impairments in cholinergic neurotransmission in the retina following BoNT/A delivery to the tectum.

Discussion

The data presented in this article provide the first evidence for structural and functional alterations in synaptic terminals distant from the site of BoNT/A injection.

Three main findings are reported: (i) BoNT/A effects can propagate retrogradely at least two synapses away from the injection site, as shown by immunolabelling for cleaved SNAP-25 in photoreceptors and rod bipolar cells following toxin injection into the tectum; (ii) cleaved SNAP-25-positive boutons in the retina are enlarged and display a higher number of synaptic vesicles, consistent with a deficit in exocytosis; (iii) a functional assay demonstrates reduced cholinergic neurotransmission-driven activity, indicating deficits in exocytosis in retinal intoxicated synapses.

Previous studies have hinted at long-distance effects of BoNT/A (10,12,27–30). Several neurophysiological data indicate central actions of BoNT/A when injected intramuscularly at therapeutic doses in humans (13,31). For example, in patients with dystonia, BoNT/A restores a normal presynaptic inhibition between forearm antagonist muscles (29). Classically, these effects have been attributed to indirect, plastic rearrangements following peripheral blockade of neurotransmission and decreased spindle afferent input to the spinal cord (15). Other studies have indicated the possibility of direct central effects of high doses of BoNT/A via long-range axonal transport and transcytosis (reviewed in 16). In particular, radiolabelled BoNT/A is transported to spinal segments after intramuscular delivery in cats (12,32). BoNT/A moves in the retrograde direction when applied at high doses in compartmented cultures of rat sympathetic neurons (33).

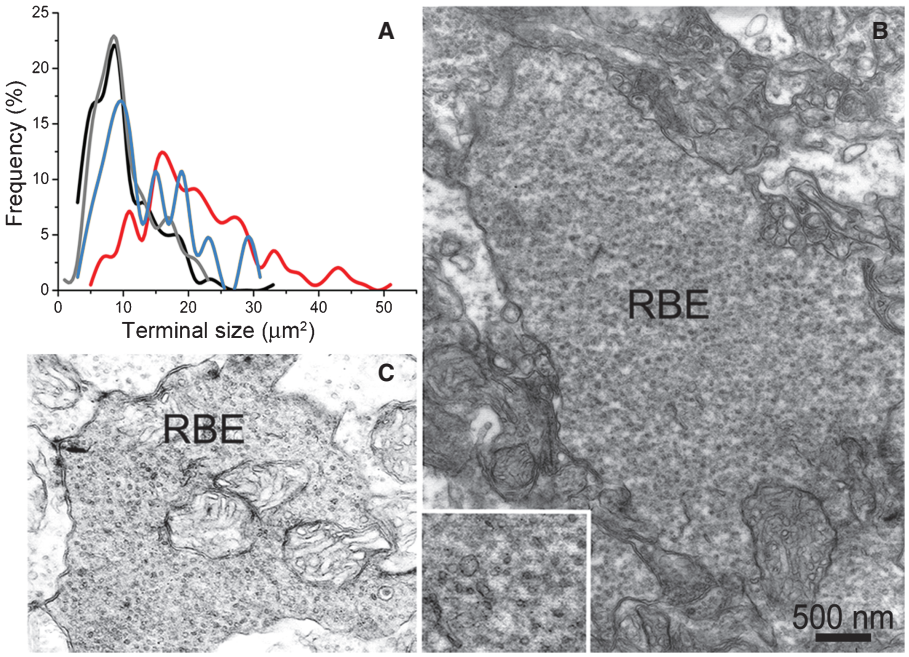

Figure 3: Morphological changes in retinal synapses after distant delivery of BoNT/A. A) Distribution of terminal sizes of rod bipolar cells. Black line, boutons from naïve, uninjected animals ($n = 202$ terminals from four rats); grey line, cleaved SNAP-25-negative terminals from BoNT/A-treated animals ($n = 107$ terminals from four rats); blue line, cleaved SNAP-25-positive terminals 3 days after BoNT/A ($n = 104$ terminals from four rats); red line, cleaved SNAP-25-positive terminals 15 days after BoNT/A ($n = 197$ terminals from five rats). B,C) Electron microscopy images of enlarged (B) and normal (C) rod bipolar cell endings (RBE) within the same retina. Inset: at twice the magnification of panels B–C, synaptic vesicles appear as the main constituent of the rod bipolar endings.

Application of BoNT/A into the rat whisker pad results in SNAP-25 cleavage within the facial nucleus (10). In cats, ultrastructural and electrophysiological changes in brainstem motoneurons were found after intramuscular BoNT/A (27,28). However, it remained unclear whether the toxin can directly impact on neurotransmission in distant districts. A recent manuscript reported no effect on neurotransmission at cell bodies when BoNT/A was applied to the peripheral chamber of compartmented cultures of sympathetic neurons (33). However, this system is quite peculiar as it lacks second-order neurons (distinct from those that uptake the toxin), in which distant effects of BoNT/A can be reliably evaluated. Here, we have exploited the excellent knowledge of visual system circuitry to demonstrate long-distance impairments in neuroexocytosis, as shown by the correspondence between SNAP-25 cleavage and structural/functional modifications of retinal cells.

Our previous studies in the visual system have demonstrated retrograde and anterograde axonal trafficking of BoNT/A, followed by transcytosis within connected neurons (10,18). The present work provides novel evidence on the features of BoNT/A trafficking. In particular, we report the first demonstration of a conspicuous BoNT/A spread within distant networks after axonal transport. Retinal circuitry has been studied in great detail (20,34,35), and we took advantage of this knowledge to map BoNT/A trafficking within retinal cells following long-range transport from the superior colliculus. The finding of cleaved SNAP-25 in photoreceptors and rod bipolar cells after tectal delivery of BoNT/A demonstrates that the toxin can affect neurons even two synapses away from the injection site. Indeed, these cells are not directly connected with retinal ganglion cells and may be exposed to the toxin only via amacrines and cone bipolars (19,36). These data suggest the occurrence of sequential cycles of transport/transcytosis of the toxin within a neuronal network. Transfer across multiple synapses has previously been described for certain neurotrophins, wheat germ agglutinin, tetanus toxin and several pathogens and virulence factors (37–39).

We also wanted to document morphological and functional consequences of SNAP-25 cleavage in retinal synaptic boutons. For the anatomical analysis, we concentrated on the terminals of rod bipolar cells in the inner plexiform layer. These terminals are sufficiently large to be amenable to confocal analysis, and are easily detectable in electron microscopy preparations (19,21). We found that rod bipolar endings positive for BoNT/A-truncated SNAP-25 were clearly enlarged as compared to control terminals within the same retina. This enlargement was significant at 3 days but became particularly evident 15 days after toxin injection, in keeping with the idea of a progressive cumulative effect. At the electron microscopy level, retinas from BoNT/A injected-rats showed rod bipolar terminals of unusually large size, characterized by a large complement of synaptic vesicles. These findings are suggestive of a continuing supply of synaptic vesicles arriving at rod bipolar endings and unable to release their neurotransmitter, with consequent increase in terminal size. A recent study has reported the appearance of large axonal swellings in the rat striatum after local delivery of BoNT/A (40). These varicosities could correspond to swollen synaptic endings, as they contained the biosynthetic enzymes for acetylcholine and dopamine (40).

To investigate functional changes triggered by retrograde BoNT/A, we measured calcium waves in the retinas of pups injected with BoNT/A into the tectum. In a

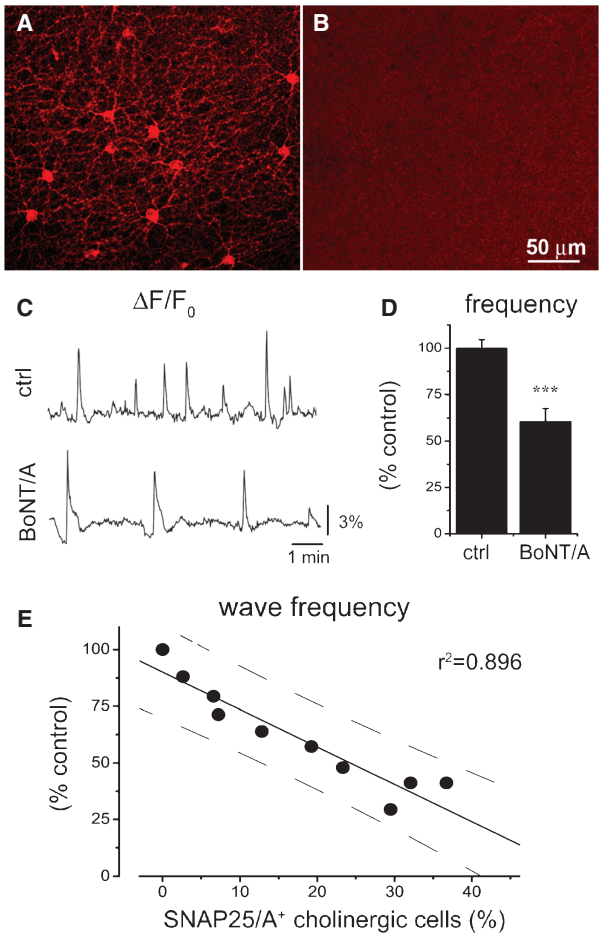

Figure 4: Reduced cholinergic-driven retinal activity following tectal administration of BoNT/A. A,B) Retinal wholemounts showing cholinergic amacrine cells immunostained for BoNT/A-truncated SNAP-25 (red) in pups with tectal injection of BoNT/A (A). No staining is detected in pups injected into the frontal cortex (B). C) Examples of calcium waves in the ganglion cell layer of a P2 control retina (ctrl) and a retina of a P2 rat injected with BoNT/A into the tectum at P0 (BoNT/A). D) Frequency of retinal waves is significantly decreased in BoNT/A-treated animals as compared to age-matched controls (ctrl; *t*-test, $p < 0.001$). Data are mean ±SE. E) The frequency of retinal waves is negatively correlated to the number of retinal cholinergic cells immunopositive for BoNT/A-truncated SNAP-25 (SNAP25/A$^+$ cholinergic cells) in P2–P8 rat pups injected with BoNT/A into the tectum (correlation coefficient $r^2 = 0.896$).

previous study, we used extracellular recordings of spiking activity to show reduced spontaneous firing in the hippocampus contralateral to BoNT/A delivery (10). However, because of bidirectional commissural connections linking the two hippocampi, it remained unclear whether this diminished spiking was due to anterograde or retrograde propagation of BoNT/A effects. Here, we have exploited the unidirectional projection from the retina to the tectum to provide evidence that the distant impairments in neurotransmission are ascribable to retrograde axonal transport and transcytosis of BoNT/A.

Retinal waves are critically dependent upon cholinergic neurotransmission during an early phase of development (25). Thus, we employed retinal waves as a readout of transmitter release from amacrine starbust cells, which are a major target of BoNT/A in the retina. We documented a robust decrease in wave frequency in the BoNT/A-treated animals, pointing to impaired acetylcholine release. This decrease in wave frequency correlated with the density of BoNT/A-truncated SNAP-25-positive starbust cells in individual retinas, further strengthening the link between SNAP-25 cleavage and the magnitude of functional changes.

In conclusion, these data provide the first evidence for the functional effects of BoNT/A retrograde trafficking. This knowledge is important to target BoNT/A as a therapeutic drug to neuronal circuits. These results also raise the possibility of using BoNT/A fragments as a drug delivery vehicle targeting specific neuronal populations in the central nervous system (37,41). This strategy was previously proposed for the non-toxic neuronal binding domain of tetanus toxin (42,43) but translation to clinical use is not feasible because of general immunization of population against tetanus. Use of non-toxic BoNT/A derivatives may avoid this limitation and provide a new class of carriers for delivery of therapeutic agents into the central nervous system.

Materials and Methods

Long-Evans hooded rats bred in our animal facility were used in this study. A total of 22 adult animals and 26 pups were used. Animals were housed in a 12 h light/dark cycle with food and water available *ad libitum*. All experimental procedures were in conformity to the European Communities Council Directive n° 86/609/EEC and were approved by the Italian Ministry of Health.

BoNT/A injections

BoNT/A was prepared and tested as described previously (10,18,44,45). Stereotaxic injections of BoNT/A or vehicle were performed unilaterally into the superior colliculus (or frontal cortex) by a glass micropipette connected to an injector (10,18,46,47). For adult rats, volume injected was 0.3 μL (2 nM solution in PBS containing 2% rat serum albumin). In P0–P2 rats, 1 nM BoNT/A was used (volume injected, 0.2 μL).

Immunohistochemistry

Adult rats were deeply anaesthetized with intraperitoneal injections of chloral hydrate (12.5% solution; 4 mL/kg) and the eyes were quickly enucleated and immersion fixed for 1 h in 4% paraformaldehyde in 0.1 M sodium phosphate buffer (PB) (pH 7.4).

The eyes were then rinsed in buffer, infiltrated overnight in 30% sucrose in 0.1 M PB, embedded in OCT/Tissue Tek (Sakura Finetek), and frozen on a cryostat stage at −30°C. Eyes were sectioned vertically in 12–16 μm serial sections with a Leica cryostat. Sections were collected on Superfrost Plus slides and air dried for 2 h. Immunostaining was performed as described (48–50). Slides were rinsed for 10 min with 0.01 M PBS and blocked for 2 h in a solution containing 10% normal goat serum, 1% bovine serum albumin (BSA) and 0.5% Triton X-100 in PBS. Primary and secondary antibodies were diluted in 3% normal goat serum, 1% BSA and 0.5% Triton X-100 in PBS. Slides were incubated in primary antibodies for

12–18 h at 4°C. After rinsing, sections were incubated for 2 h in solutions containing appropriate secondary antibodies diluted 1:400, and conjugated with Oregon Green 488, Alexa Fluor 568 (Invitrogen), or Rhodamine Red-X (Jackson ImmunoResearch Laboratories).

Primary antibodies and dilutions were as follows: polyclonal antibody raised against the BoNT/A truncated C-terminal peptide of SNAP-25, 1:500 (kind gift of Dr. Rossetto, University of Padua, Italy; 10, 17, 18); monoclonal anti-protein kinase C α (PKC α), 1:1000, clone MC5 (Sigma P5704).

In pups, immunohistochemistry was performed on retinal wholemounts according to published protocols (51). Briefly, at the end of the calcium wave recording session, retinas were fixed in 4% PFA, rinsed and processed as described for retinal sections increasing the incubation times to 12 h for blocking solution, 4 days for primary antibody and 2 days for secondary antibody.

Sections were scanned with a Leica TCS-NT confocal microscope (Leica Microsystems) equipped with an Argon-Krypton laser, at resolutions of 1024 × 1024 pixels. Images were obtained using a 40× HCX PL APO 1.25× oil objective.

Morphometric analyses

Retinal samples from rats injected with BoNT/A in the superior colliculus were isolated 3 and 15 days after the injections, sectioned vertically at the cryostat and stained with SNAP-25 and PKC antibodies as explained above. The sections were scanned at the confocal microscope to include the inner plexiform layer and the synaptic terminals of rod bipolar cells. Images were exported in tiff format on a computer station equipped with Metamorph for image analysis. The diameter and area of synaptic endings of rod bipolar cells (both double labelled and stained with PKC antibodies only) were measured by the appropriate Metamorph graphic tools.

For the analysis of cleaved SNAP-25-positive retinal neurons, cells were counted on 63 randomly chosen vertical sections from four retinas of animals that received tectal BoNT/A injection 3–15 days before. Cleaved SNAP-25-positive neurons were divided into four types: rod bipolars (RB, PKC positive), cone bipolars (CB, PKC negative), amacrine cells (AC) and photoreceptor cells (Ph), the latter two are identified on the basis of their position and typical morphology. A total of 416 cells were counted.

Electron microscopy

Eye cups dissected as mentioned above were fixed in 2.5% glutaraldehyde, 2% paraformaldehyde for 8 h at 4°C. Retinal fragments (3 × 2 mm) were dissected with a sharp blade, postfixed in 1% osmium tetroxide, stained *en bloc* with uranyl acetate, dehydrated in ethanol and embedded in Epon–Araldite plastic for electron microscopy. Ultrathin vertical sections were stained with uranyl acetate and lead citrate and examined with a Jeol 1200 EXII electron microscope. Micrographs of the innermost lamina of the inner plexiform layer were taken at various magnification, developed and scanned with a Nikon high resolution scanner for subsequent examination (21,36).

Calcium waves recording

Retinas were prepared as described (51). After decapitation, eyes were enucleated, retinas isolated in oxygenated ACSF (NaCl 119 mM, KCl 2.5 mM, $MgCl_2$ 1.30 mM, $CaCl_2$ 2.5 mM, NaH_2PO_4 1 mM, glucose 11 mM, HEPES 20 mM), flat-mounted ganglion cell layer side up onto a black filter (Millipore) and incubated for 1 h in oxygenated ACSF with 0.005% pluronic acid, 1% DMSO and 1% Oregon Green BAPTA-1AM (OGB-1AM, Invitrogen) or Calcium Orange AM (CO AM, Invitrogen) at 34°C. After rinsing, retinas were placed in a 2-mL incubation chamber on the stage of an epifluorescence microscope (Zeiss Axioskop 2 FS plus). The chamber was perfused with oxygenated ACSF (90 mL/h) maintained at 34°C by a controller acting on the chamber and the perfusion line (Warner System). Images were acquired with a CCD camera (C3Plus, DTA), using 10×, 20× or 40× water immersion UMPlanFI objectives (Olympus). Exposure time was 100 milliseconds and frame rate 1.4 Hz.

Calcium image analysis and wave detection

The fluorescence intensity associated to the calcium indicator was measured in selected $100 \times 100\,\mu m^2$ regions within a $1.5 \times 1\,mm^2$ sampling field. In each region, the average fluorescence intensity as a function of time, $F(t)$, was measured with MetaMorph (Molecular Devices). To correct for dye bleaching over time, the relative change in fluorescence intensity $\Delta F/F_0(t)$ was used, where $\Delta F = F(t) - F_0(t)$, and $F_0(t)$ is the baseline fluorescence intensity. Wave frequency per retina was defined as the inverse of the average of the intervals separating two consecutive waves in the recording.

Statistical analysis

Data are reported as mean ± SE. Differences between two groups were assessed with Student's *t*-test. Differences between terminal size distributions of rod bipolar cells were assessed by Kolmogorov-Smirnov test (K-S test). Statistical analysis was performed using SigmaStat (Systat), correlation analysis using Origin (Microcal).

Acknowledgments

This work was supported by the Italian Ministry of Health (PRIN – Progetti di Rilevante Interesse Nazionale – 2008) and by Tuscany region (Health Program 2009). We thank Dr. Ornella Rossetto (University of Padua) for providing antibodies against cleaved SNAP-25, and Lamberto Maffei for critical reading of the manuscript. None of the authors has conflicts of interest to disclose.

References

1. Johnson EA. Clostridial toxins as therapeutic agents: benefits of nature's most toxic proteins. Annu Rev Microbiol 1999;53:551–575.
2. Schiavo G, Matteoli M, Montecucco C. Neurotoxins affecting neuroexocytosis. Physiol Rev 2000;80:717–766.
3. Rossetto O, Morbiato L, Caccin P, Rigoni M, Montecucco C. Presynaptic enzymatic neurotoxins. J Neurochem 2006;97:1534–1545.
4. Davletov B, Bajohrs M, Binz T. Beyond BOTOX: advantages and limitations of individual botulinum neurotoxins. Trends Neurosci 2005;28:446–452.
5. Montecucco C, Molgo J. Botulinal neurotoxins: revival of an old killer. Curr Opin Pharmacol 2005;5:274–279.
6. Montal M. Botulinum neurotoxin: a marvel of protein design. Annu Rev Biochem 2010;79:591–617.
7. Simpson DM, Blitzer A, Brashear A, Comella C, Dubinsky R, Hallett M, Jankovic J, Karp B, Ludlow CL, Miyasaki JM, Naumann M, So Y. Assessment: botulinum neurotoxin for the treatment of movement disorders (an evidence-based review): report of the Therapeutics and Technology Assessment Subcommittee of the American Academy of Neurology. Neurology 2008;70:1699–1706.
8. Simpson DM, Gracies JM, Graham HK, Miyasaki JM, Naumann M, Russman B, Simpson LL, So Y. Assessment: botulinum neurotoxin for the treatment of spasticity (an evidence-based review): report of the Therapeutics and Technology Assessment Subcommittee of the American Academy of Neurology. Neurology 2008;70:1691–1698.
9. Naumann M, So Y, Argoff CE, Childers MK, Dykstra DD, Gronseth GS, Jabbari B, Kaufmann HC, Schurch B, Silberstein SD, Simpson DM. Assessment: botulinum neurotoxin in the treatment of autonomic disorders and pain (an evidence-based review): report of the Therapeutics and Technology Assessment Subcommittee of the American Academy of Neurology. Neurology 2008;70:1707–1714.
10. Antonucci F, Rossi C, Gianfranceschi L, Rossetto O, Caleo M. Long-distance retrograde effects of botulinum neurotoxin A. J Neurosci 2008;28:3689–3696.

11. Moreno-Lopez B, de la Cruz RR, Pastor AM, Delgado-Garcia JM. Botulinum neurotoxin alters the discharge characteristics of abducens motoneurons in the alert cat. J Neurophysiol 1994;72:2041–2044.
12. Wiegand H, Erdmann G, Wellhoner HH. 125I-labelled botulinum A neurotoxin: pharmacokinetics in cats after intramuscular injection. Naunyn Schmiedebergs Arch Pharmacol 1976;292:161–165.
13. Gracies JM. Physiological effects of botulinum toxin in spasticity. Mov Disord 2004;19(Suppl. 8):S120–S128.
14. Caleo M, Antonucci F, Restani L, Mazzocchio R. A reappraisal of the central effects of botulinum neurotoxin type A: by what mechanism? J Neurochem 2009;109:15–24.
15. Curra A, Berardelli A. Do the unintended actions of botulinum toxin at distant sites have clinical implications? Neurology 2009;72: 1095–1099.
16. Caleo M, Schiavo G. Central effects of tetanus and botulinum neurotoxins. Toxicon 2009;54:593–599.
17. Matak I, Bach-Rojecky L, Filipovic B, Lackovic Z. Behavioral and immunohistochemical evidence for central antinociceptive activity of botulinum toxin A. Neuroscience 2011;186:201–207.
18. Restani L, Antonucci F, Gianfranceschi L, Rossi C, Rossetto O, Caleo M. Evidence for anterograde transport and transcytosis of botulinum neurotoxin A (BoNT/A). J Neurosci 2011;31:15650–15659.
19. Chun MH, Han SH, Chung JW, Wassle H. Electron microscopic analysis of the rod pathway of the rat retina. J Comp Neurol 1993;332: 421–432.
20. Masland RH. The fundamental plan of the retina. Nat Neurosci 2001;4:877–886.
21. Strettoi E, Dacheux RF, Raviola E. Synaptic connections of rod bipolar cells in the inner plexiform layer of the rabbit retina. J Comp Neurol 1990;295:449–466.
22. Stacy RC, Demas J, Burgess RW, Sanes JR, Wong RO. Disruption and recovery of patterned retinal activity in the absence of acetylcholine. J Neurosci 2005;25:9347–9357.
23. Penn AA, Riquelme PA, Feller MB, Shatz CJ. Competition in retinogeniculate patterning driven by spontaneous activity. Science 1998;279:2108–2112.
24. Torborg CL, Feller MB. Spontaneous patterned retinal activity and the refinement of retinal projections. Prog Neurobiol 2005;76:213–235.
25. Wong RO, Meister M, Shatz CJ. Transient period of correlated bursting activity during development of the mammalian retina. Neuron 1993;11: 923–938.
26. Galli L, Maffei L. Spontaneous impulse activity of rat retinal ganglion cells in prenatal life. Science 1988;242:90–91.
27. Moreno-Lopez B, de la Cruz RR, Pastor AM, Delgado-Garcia JM. Effects of botulinum neurotoxin type A on abducens motoneurons in the cat: alterations of the discharge pattern. Neuroscience 1997;81: 437–455.
28. Pastor AM, Moreno-Lopez B, De La Cruz RR, Delgado-Garcia JM. Effects of botulinum neurotoxin type A on abducens motoneurons in the cat: ultrastructural and synaptic alterations. Neuroscience 1997; 81:457–478.
29. Priori A, Berardelli A, Mercuri B, Manfredi M. Physiological effects produced by botulinum toxin treatment of upper limb dystonia. Changes in reciprocal inhibition between forearm muscles. Brain 1995; 118(Pt 3):801–807.
30. Wiegand H, Wellhoner HH. The action of botulinum A neurotoxin on the inhibition by antidromic stimulation of the lumbar monosynaptic reflex. Naunyn Schmiedebergs Arch Pharmacol 1977;298:235–238.
31. Abbruzzese G, Berardelli A. Neurophysiological effects of botulinum toxin type A. Neurotox Res 2006;9:109–114.
32. Habermann E. 125I-labeled neurotoxin from Clostridium botulinum A: preparation, binding to synaptosomes and ascent to the spinal cord. Naunyn Schmiedebergs Arch Pharmacol 1974;281:47–56.
33. Lawrence GW, Ovsepian SV, Wang J, Aoki KR, Dolly JO. Extravesicular intraneuronal migration of internalized botulinum neurotoxins without detectable inhibition of distal neurotransmission. Biochem J 2012;441:443–452.
34. Wassle H. Parallel processing in the mammalian retina. Nat Rev Neurosci 2004;5:747–757.
35. Jeon CJ, Strettoi E, Masland RH. The major cell populations of the mouse retina. J Neurosci 1998;18:8936–8946.
36. Strettoi E, Raviola E, Dacheux RF. Synaptic connections of the narrow-field, bistratified rod amacrine cell (AII) in the rabbit retina. J Comp Neurol 1992;325:152–168.
37. Salinas S, Schiavo G, Kremer EJ. A hitchhiker's guide to the nervous system: the complex journey of viruses and toxins. Nat Rev Microbiol 2010;8:645–655.
38. von Bartheld CS, Wang X, Butowt R. Anterograde axonal transport, transcytosis, and recycling of neurotrophic factors: the concept of trophic currencies in neural networks. Mol Neurobiol 2001;24:1–28.
39. Rind HB, Butowt R, von Bartheld CS. Synaptic targeting of retrogradely transported trophic factors in motoneurons: comparison of glial cell line-derived neurotrophic factor, brain-derived neurotrophic factor, and cardiotrophin-1 with tetanus toxin. J Neurosci 2005;25:539–549.
40. Wree A, Mix E, Hawlitschka A, Antipova V, Witt M, Schmitt O, Benecke R. Intrastriatal botulinum toxin abolishes pathologic rotational behaviour and induces axonal varicosities in the 6-OHDA rat model of Parkinson's disease. Neurobiol Dis 2011;41:291–298.
41. von Bartheld CS. Axonal transport and neuronal transcytosis of trophic factors, tracers, and pathogens. J Neurobiol 2004;58:295–314.
42. Bizzini B, Grob P, Glicksman MA, Akert K. Use of the B-IIb tetanus toxin derived fragment as a specific neuropharmacological transport agent. Brain Res 1980;193:221–227.
43. Francis JW, Bastia E, Matthews CC, Parks DA, Schwarzschild MA, Brown RH Jr, Fishman PS. Tetanus toxin fragment C as a vector to enhance delivery of proteins to the CNS. Brain Res 2004;1011:7–13.
44. Costantin L, Bozzi Y, Richichi C, Viegi A, Antonucci F, Funicello M, Gobbi M, Mennini T, Rossetto O, Montecucco C, Maffei L, Vezzani A, Caleo M. Antiepileptic effects of botulinum neurotoxin E. J Neurosci 2005;25:1943–1951.
45. Schiavo G, Montecucco C. Tetanus and botulism neurotoxins: isolation and assay. Methods Enzymol 1995;248:643–652.
46. Caleo M, Menna E, Chierzi S, Cenni MC, Maffei L. Brain-derived neurotrophic factor is an anterograde survival factor in the rat visual system. Curr Biol 2000;10:1155–1161.
47. Tropea D, Caleo M, Maffei L. Synergistic effects of brain-derived neurotrophic factor and chondroitinase ABC on retinal fiber sprouting after denervation of the superior colliculus in adult rats. J Neurosci 2003; 23:7034–7044.
48. Gargini C, Terzibasi E, Mazzoni F, Strettoi E. Retinal organization in the retinal degeneration 10 (rd10) mutant mouse: a morphological and ERG study. J Comp Neurol 2007;500:222–238.
49. Strettoi E, Volpini M. Retinal organization in the bcl-2-overexpressing transgenic mouse. J Comp Neurol 2002;446:1–10.
50. Mazzoni F, Novelli E, Strettoi E. Retinal ganglion cells survive and maintain normal dendritic morphology in a mouse model of inherited photoreceptor degeneration. J Neurosci 2008;28:14282–14292.
51. Resta V, Novelli E, Di Virgilio F, Galli-Resta L. Neuronal death induced by endogenous extracellular ATP in retinal cholinergic neuron density control. Development 2005;132:2873–2882.